RSC Advances

ROYAL SOCIETY OF CHEMISTRY

www.rsc.org/advances

RSC Advances

An international journal to further the chemical sciences

RSC Advances is an international, peer-reviewed, online journal covering all of the chemical sciences, including interdisciplinary fields.

The **criteria for publication** are that the experimental and/ or theoretical work must be **high quality**, **well conducted** and **demonstrate an advance by adding to the development of the field**

***RSC Advances* 2013 Impact Factor* = 3.7**

Thank you for your assistance in evaluating this manuscript.

Guidelines to the referees

Referees have the responsibility to treat the manuscript as confidential. Please be aware of our Ethical Guidelines, which contain full information on the responsibilities of referees and authors, and our Refereeing Procedure and Policy.

It is essential that all research work reported in *RSC Advances* is well-carried out and well-characterised. There should be enough supporting evidence for the claims made in the manuscript.

When preparing your report, please:

- comment on the originality and scientific reliability of the work;
- comment on the characterisation of the compounds/materials reported - has this has been accurately interpreted and does it support the conclusions of the work;
- state clearly whether you would like to see the article accepted or rejected and give detailed comments (with references, as appropriate) that will both help the Editor to make a decision on the article and the authors to improve it.

Please inform the Editor if:

- there is a conflict of interest
- there is a significant part of the work which you are not able to referee with confidence
- the work, or a significant part of the work, has previously been published
- you believe the work, or a significant part of the work, is currently submitted elsewhere
- the work represents part of an unduly fragmented investigation.

For further information about *RSC Advances*, please visit: www.rsc.org/advances or contact us by email: advances@rsc.org.

*Data based on 2013 Journal Citation Reports®, (Thomson Reuters, 2014).

Journal Name

RSCPublishing

ARTICLE

Controllable Synthesis of Fluorapatite Microcrystals Decorated with Silver Nanoparticles and Their Optical Property

Cite this: DOI: 10.1039/x0xx00000x

Received 00th January 2014,
Accepted 00th January 2014

DOI: 10.1039/x0xx00000x

www.rsc.org/

Di Li[a], Deli Jiang[b,*], Jimin Xie[b]

An EDTA-assisted hydrothermal method is developed for the controlled preparation of fluorapatite microcrystals (FHAp MPs) decorated with silver nanoparticles (Ag NPs). The synthesis process involves the use of EDTA as both a chelating agent and a reducing agent, allowing the one-pot formation of Ag/FHAp composites. The resultant product was characterized by X-ray diffraction pattern (XRD), field emission scanning electron micrograph (FESEM), transmission electron microscopy (TEM), and UV−vis diffuse reflection spectroscopy (UV-DRS). The Ag NPs prepared via this method exhibit monodispersed size distribution and essentially uniform dispersion on FHAp MPs supports. It was demonstrated that the morphology of FHAp MPs can be tuned by varying the concentration of silver nitrate in the starting reaction solution, or by varying the pH value of reaction solution. A possible growth mechanism was discussed for the formation of Ag/FHAp composites. Additionally we also demonstrated that the resulting Ag/FHAp composites with different Ag loadings possess tunable optical properties.

1. Introduction

Ever since the great advance in the synthesis of single-component colloidal nanocrystals with controlled sizes and shapes, there has been growing attention in the development of nanocomposite materials, which combine two- or more functional components and could provide novel properties beyond each individual component.[1–3] In recent years, silver nanoparticles (Ag NPs) and silver-containing composite materials have garnered substantial interest for many applications including catalysis, surface enhanced Raman scattering (SERS), optoelectronics, and biomedicine.[4–8] Hydroxyapatite [HAp; $Ca_{10}(PO_4)_6(OH)_2$] and their F-substituted counterparts (FHAp) are principle inorganic constituents of animal bones and teeth.[9,10] Artificially synthesized HAp and FHAp are widely used in biomedical fields, catalyst, sensors, fluorescencematerials, chromatography, and environmental phosphorus recovery.[11–19] Among the various investigated silver-containing hybrid materials, HAp and FHAp supported Ag NPs composites have been of particular interest.[20,21] Recent studies by Kaneda et al. have revealed that HAp-supported Ag NPs exhibit high catalytic activity for the selective oxidation of various phenylsilanes into phenylsilanols in water[22] and selective hydration of nitriles to amides in aqueous solution.[23] In another field, HAp-supported Ag NPs have been reported to be potential antibacterial agents due to the well-known biocompatibility of HAp and antibacterial activity of nanosilver.[24,25]

Up to now, supported Ag NPs have often been obtained by a two-step wet chemical protocol.[22-24,26] This involves the deposition of molecular or ionic precursors, such as $AgNO_3$, on the desired support from the aqueous or organic liquid phase, followed by the reduction with suitable reducing agents, such as hydrogen or potassium borohydride.[22-24] However, it is recognized that reduction of silver ions in the presence of H_2 (or $NaBH_4$), which on an industrial scale is dangerous due to the volatile nature of the H_2 gas. Moreover, it is difficult to have a complete control on all parameters in a multistep process and therefore, reproducible results are not easily achievable. The development of synthetic routes allowing Ag NPs fabrication in direct conjunction with the desired support in one single-step is highly desirable and remains a great challenge.

In this work, a facile strategy for the single-step fabrication of FHAp MPs decorated with Ag NPs was presented. This approach employs EDTA as both a chelating agent and a reducing agent, which allows the in situ reduction of Ag NPs and simultaneous formation of FHAp MPs, leading to the formation of Ag/FHAp composites. It was found that the loading amount of Ag NPs and the morphology of FHAp MPs can be controlled by varying the concentration of silver nitrate in the starting reaction solution or varying the solution pH value. Compared to the previously reported multistep synthetic routes, the current synthesis process is facile, cost-effective and it is easy to handle, and thus might even be scalable for the production of FHAp-supported Ag NPs. Furthermore, the as prepared Ag/FHAp composites with different Ag loadings exhibit tunable surface plasmon resonance properties.

2. Experimental Section

2.1. Materials

Ethylenediaminetetraacetic disodium salt (Na_2EDTA), silver nitrate ($AgNO_3$), calcium nitratetetrahydrate ($Ca(NO_3)_2{\cdot}4H_2O$), diammonium hydrogen phosphate ($(NH_4)_2HPO_4$), sodium hydroxide (NaOH) and nitric acid (HNO_3) were purchased from Sinopharm Chemical Reagent Co., Ltd., China and used as-received without any further purification.

2.2. Synthesis of Ag/FHAp Composites

To fabricate Ag/FHAp composites, 5 mmol of Na_2EDTA was first dissolved in 50 mL of distilled water until it became a clear solution. Then 5 mmol of $Ca(NO_3)_2{\cdot}4H_2O$, 3 mmol of $(NH_4)_2HPO_4$, and a varied amount of $AgNO_3$ were added into the above clear solution. The pH value of resulting mixture was adjusted to 3.7 using NaOH (0.1 M) and HNO_3 (0.1 M), followed by the addition of 1.5 mmol of NaF. After being stirred for 10 min, the mixture was transferred into a 20-mL Teflon-lined stainless autoclave and kept at 160 °C for 8 h. The resultant off-white precipitate was then collected, washed, and dried in an oven of 60 °C before characterization. The silver loading (*x*) was chosen as 1.25, 2.5, 5.0, which was the mole percentage of silver element in the theoretical Ag/FHAp samples. The obtained samples with corresponding silver loadings were denoted as Ag*x*/FHAp. The pure FHAp sample was synthesized by the same procedure, except no $AgNO_3$ was added.

2.3. Characterization

The phase purity and crystal structure of the obtained samples were examined by X-ray diffraction (XRD) using D8 Advance X-ray diffraction (Bruker axs company, Germany). The morphology of the as-prepared samples was examined by a field emission scanning electron micrograph (FESEM) instrument (Hitachi S-4800 II, Japan). Transmission electron microscopy (TEM) was recorded on a JEOL-JEM-2010 (JEOL, Japan) operating at 120 kV. UV−vis diffuse reflection spectroscopy (UV-DRS) was performed on a Shimadzu UV-3100 spectrophotometer using $BaSO_4$ as the reference.

3. Results and Discussion

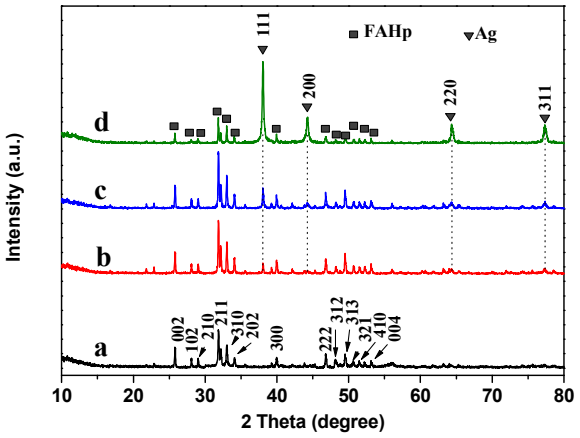

Fig. 1 XRD patterns of (a) FHAp, (b) Ag1.25/FHAp, (c) Ag2.5/FHAp, and (d) Ag5/FHAp samples.

Fig. 1 shows the XRD patterns of FHAp MPs and Ag/FHAp hybrid samples with different silver loadings. All the diffraction peaks in Fig. 1(a) can be indexed to the hexagonal phase of FHAp (JCPDS No. 00-015-0876). With the addition of small amount of $AgNO_3$ salt, the as-synthesized Ag1.25/FHAp sample is predominantly composed of FHAp, along with a detectable silver phase with face-centered cubic (fcc) structure (Fig. 1(b)). As more $AgNO_3$ salt is added, the evolution of the diffraction peaks from fcc silver is clearly seen for Ag2.5/FHAp and Ag5/FHAp sample, as shown in Fig. 1(c) and (d). For all these as-synthesized Ag/FHAp hybrid samples, no characteristic diffraction peaks assigned to the Ag_2O phase can be found in the corresponding XRD patterns, revealing that the present single-step synthesis process can avoid the oxidation of silver ion.

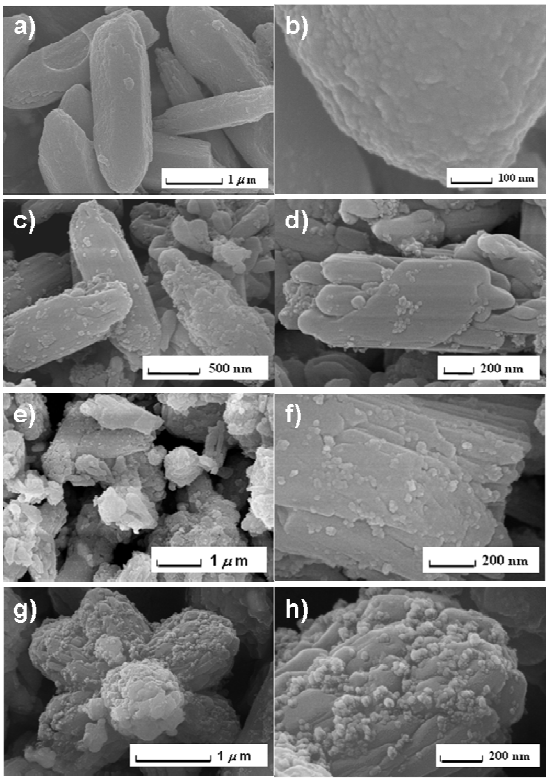

Fig. 2 FESEM images of (a,b) FHAp, (c,d) Ag1.25/FHAp, (e,f) Ag2.5/FHAp, and (g,h) Ag5/FHAp samples.

The morphology of FHAp MPs and Ag/FHAp samples with different silver loadings were first characterized by FESEM. As shown in Fig. 2(a) and (b), without $AgNO_3$, the prepared sample is composed of rod-like FHAp MPs with lengths ranging from 2 to 4 μm. No Ag NPs can be observed on the surface of FHAp MPs. When $AgNO_3$ was introduced in the reaction solution, Ag NPs supported on FHAp MPs were obtained. As shown in the corresponding FESEM images for the Ag1.25/FHAp sample, rod-like FHAp MPs with size ranging from 1 to 2 μm decorated with Ag NPs with average size of around 26 nm were generated. For Ag2.5/FHAp and Ag5/FHAp samples, the loadings of silver on the surface of FHAp increase with increasing the concentration of silver nitrate in the starting reaction solution. In addition, one can observe from the Fig. 2(g) and (h) that the size distribution of Ag NPs for the Ag5/FHAp sample is the widest one among those as-prepared Ag/FHAp samples. A possible process to the Ag particle formation was proposed, as follows. Firstly, the $NH_3{\cdot}H_2O$ which hydrolysis by NH_4^+ in the reaction system will coordinate with Ag to produce the Tollens' reagent. Then, due to the existence of Na_2EDTA which could be act as light

reductant[27], the as-formed Tollens' reagent will be reduced to Ag. Meanwhile, an interesting phenomenon has been discovered, with the increasing the amount of Ag^+, the self-assembly process of the products seems to be more obviously. This is because the Ca atom which contained unsaturated ligand in FHAp surface could bond with OH^-, while the F atom also could attract the OH^- to form hydrogen bond to enhance the attraction between the products. Therefore, more OH^- existed in the reaction system, and the final products are more inclined to form a hierarchical structure. On the other hand, the Na_2EDTA might be oxidated by Tollens' reagent to produce amine oxide and the pH valve of the system will be increased which will be investigated in the following section. Thus, it was considered that the amount of Ag^+ could directly influence the amount of OH^- and ultimately affect the morphology of the FHAP.

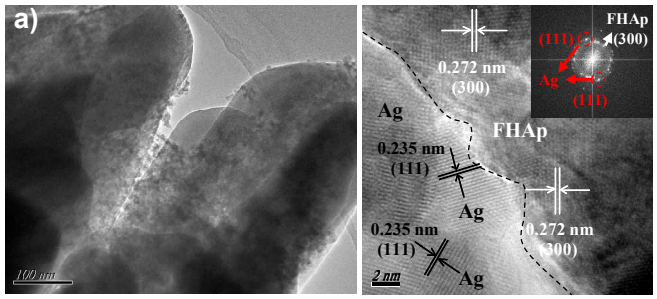

Fig. 3 (a) TEM image and (b) HRTEM image of as-synthesized Ag1.25/FHAp sample. Inset in panel b shows the corresponding FFT pattern.

To further identify the structure of Ag/FHAp composite, TEM characterization was performed on the Ag1.25/FHAp sample and was shown in Fig. 3. As shown in Fig. 3(a), it can be further confirmed that the Ag1.25/FHAp are composed by nanorods with a diameter about 300 nm, and the silver nanopartices mainly attach on the surface of FHAp microcrystal, instead of embedding into the FHAp. As shown in Figure 3(b), the high-resolution TEM (HRTEM) image and corresponding FFT pattern for the Ag1.25/FHAp hybrid indicate that the supported silver nanoparticles is enclosed by {111} facets, as can be confirmed from the lattice fringes with an interplanar distance of 0.235 nm, while the FHAp substrate particles are enclosed by {300} facets, according to the existing 0.272 nm interplanar distance.

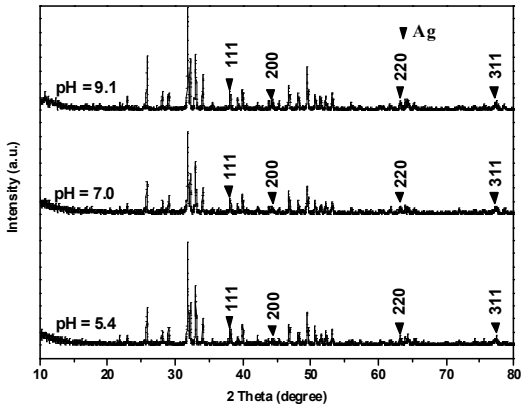

Fig. 4 XRD patterns of as-prepared Ag1.25/FHAp samples prepared at pH value of 5.4, 7.0, and 9.1, respectively.

Then, it was found that the morphologies of Ag/FHAp composites could be tuned by varying the pH value of the initial reaction solution during the experiment. Fig. 4 shows the XRD patterns of Ag1.25/FHAp samples prepared at pH value of 5.4, 7.0, and 9.1, respectively. We can found that for the three samples, all the diffraction patterns assigned to Ag phase which prove the existence of Ag obviously.

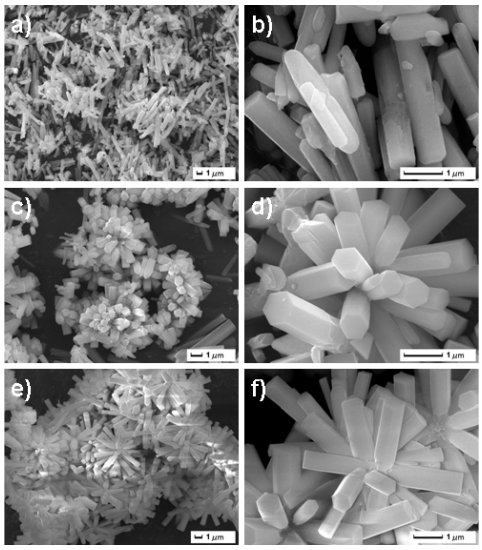

Fig. 5 FESEM images of as-prepared Ag1.25/FHAp samples prepared at different pH values: (a,b) 5.4, (c,d) 7.0, and (e,f) 9.1.

As shown in Fig. 5, Ag/FHAp composites of various morphologies were obtained at different pH values. At pH = 5.4, the FHAp appears as one-dimensional hexagonal microrods, with diameters of about 500 nm and lengths of up to several micrometers (Fig. 5(a) and (b)). In contrast, both the samples prepared at pH 7.0 and 9.1 are composed of three-dimensional flower-like microrod aggregates (Fig.5 (d) and (h)). From the magnified FESEM images (Fig. 5(e) and (i)), it can be observed that each flower-like hierarchical structure is made up of several well-defined short hexagonal FHAp microrods, which further confirms the results of previous view. Although flower-like FHAp microstructures have been reported in the literature,[28,29] the observation of flower-like microstructure constructing from hexagonal FHAp microrods is very few.

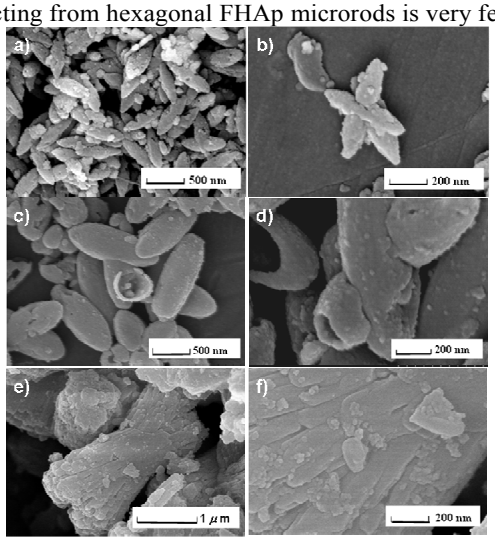

Fig. 6 FESEM images of Ag1.25/FHAp samples prepared at different reaction intervals: (a,b) 0.5 h, (c,d) 1 h, and (e,f) 4 h.

To address the growth mechanism of Ag/FHAp composites (taking Ag1.25/FHAp as an example), samples were taken out from the reaction solution at different time intervals during the hydrothermal process and the results were presented in Fig. 6. The FESEM images in Fig. 6(a) and (b) show that the sample formed in the investigated first stage was composed of shuttle-like FHAp MPs with rough surfaces, together with some visible Ag NPs with a wide size distribution (~10–50 nm). Prolonging the reaction time to 1 h led to the formation of Ag domains which are distributed on FHAp MPs (Fig. 6(c) and (d)). The Ag NPs formed at this stage have a much narrower size distribution compared with that of the sample collected after 0.5 h reaction time. Further increase in the reaction time (4 h) causes a tremendous change in the morphology of FHAp MPs; but both the size and shape of the supported Ag NPs were essentially unchanged.

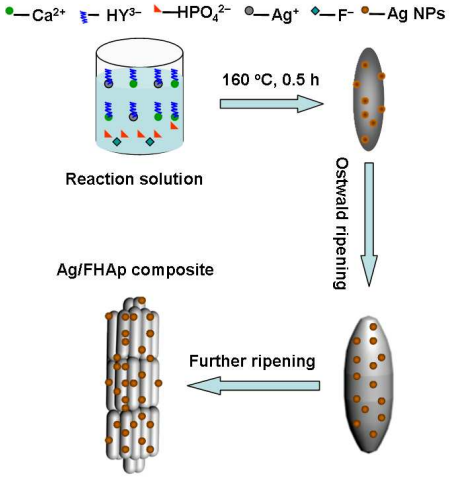

Fig. 7 Schematic illustration of the formation process of the Ag/FHAp composites.

On the basis of above results and our previous observations, a plausible growth mechanism for the Ag/FHAp composites was proposed, as shown in Fig. 7. EDTA has been widely employed as a chelating reagent in the synthesis of colloidal nanocrystals with controlled shape and size.[30] In the present case, EDTA will firstly mobilize Ca^{2+} during the first step of starting reagents mixture process to generate EDTA–Ca.[28] Upon heating up the precipitation medium, Ca^{2+} was released from the complexes mentioned above and the supersaturation condition could be achieved. The negative $H_2PO_4^-$, OH^-, and F^- in the solution then react with the free Ca^{2+} to generate FHAp nuclei. When the reaction time was 30 min, these FHAp nuclei then grow into shuttle-shaped FHAp nanoparticles along certain orientation due to the selective adsorption of anionic EDTA species and F^- on their specific surfaces. If the reaction time reaches 1 h, the size of the shuttle-shaped FHAp nanoparticles increases significantly via the Ostwald ripening mechanism. When the reaction time was 4 h, rod-like hierarchical FHAp microstructure formed with enlarged sizes as compared to the shuttle-shaped FHAp nanoparticles. When the amount of Ag^+ or pH value was further increased, the self-assembly hierarchical FHAp appeared. During these periods, Ag nuclei which produced from the Tollens' reagent would aggregate together to form primary Ag particles. Once aggregated, these Ag particles tend to adsorb on the FHAp MPs surface due to the electrostatic interaction or van der Waals forces between Ag NPs and FHAp MPs.

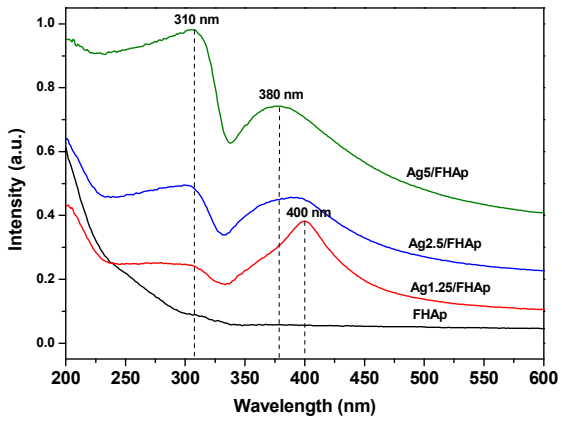

Fig. 8 UV–vis absorbance spectra of as-synthesized FHAp and Ag/FHAp composites.

The optical adsorption of Ag/FHAp composite was examined by the UV–vis DRS technique. As shown in Fig. 8, two optical adsorption bands occurring around 300–315 nm and 350–450 nm were detected in the three Ag/FHAp samples, but not in pure FHAp sample. According to previous UV–vis studies on the silver materials,[31,32] the absorption band in the region of 310–320 nm can be assigned to metallic silver film or big particles. The case of silver can be excluded by the FESEM results (Fig. 2). The Ag1.25/FHAp sample has a major absorption peak at 400 nm which can be ascribed to the characteristic of the surface plasmon resonance of Ag nanoparticles, indicating that metallic Ag NPs were formed.[33,34] In general, the intensity enhancement of absorption band results from the increase of metal particle size, combining with the band shift.[35,36] In the present case, we found that increasing the silver loadings led to a slender blue-shift in the absorption band, which can be attributed to the reduction in the silver particle size for the Ag2.5/FHAp sample. As the silver loadings increasing (for the Ag5/FHAp sample), the absorption peak was further blue-shifted to around 380 nm, which is commonly attributed to the Ag NPs aggregates and/or to the reduction in the size of Ag NPs.

Conclusions

In summary, this work shown that Ag/FHAp composites can be synthesized by a single-step hydrothermal method, where EDTA was solely used as both a chelating agent and a reducing agent. It was found that the loading of Ag NPs on the FHAp MPs and the morphology of FHAp can be controlled by varying the concentration of silver nitrate in the starting reaction solution, as well as by varying the solution pH value. In addition, the as-prepared Ag/FHAp composites with different silver loadings were found to exhibit tunable surface plasma resonance properties, depending on the synthesis conditions. Since the present single-step process is facile, cost-effective and it is easy to handle, it could be scalable for the production of FHAp-supported Ag NPs and might be tailored to other metal–FHAp systems, such as Au/FHAp.

Acknowledgements

This work was supported by the financial supports of Natural Science Foundation of Jiangsu Province (BK20140530), College Natural Science Research Program of Jiangsu Province

(13KJB610003), and Research Foundation for Talented Scholars of Jiangsu University (11JDG149).

Notes

a Institute for Energy Research, Jiangsu University, Zhenjiang 212013, China
b School of Chemistry and Chemical Engineering, Jiangsu University, Zhenjiang 212013, China; dlj@ujs.edu.cn

References

1. P. Kundu, A. Halder, B. Viswanath, D. Kundu, G. Ramanath and N. Ravishankar, *J. Am. Chem. Soc*., 2010, **132**, 20.
2. R. Costi, A. E. Saunders and U. Banin, *Angew. Chem. Int. Ed*., 2010, **49**, 4878.
3. P. D. Cozzoli, T. Pellegrino and L. Manna, *Chem. Soc. Rev*., 2006, **35**, 1195.
4. C. X. Zhang, P. Chen, J. Liu, Y. H. Zhang, W. Shen, H. L. Xu and Y. Tang, *Chem. Commun.*, 2008, **28**, 3290.
5. K. Yliniemi, M. Vahvaselka, Y. V. Ingelgem, K. Baert, B. P. Wilson, H. Terryn and K. Kontturi, *J. Mater. Chem*. 2008, **18**, 199.
6. V. Purcar, D. Donescu, C. Petcu, R. Luque and D. J. Macquarrie, *Appl. Catal. A: Gen.*, 2009, **363**, 122.
7. M. A. Syed, S. Babar, A. S. Bhatti and H. Bokhari, *J. Biomed. Nanotechnol.*, 2009, **5**, 209.
8. R. Nirmala, H. S. Kang, H. M. Park, R. Navamathavan, I.S. Jeong and H. Y. Kim, *J. Biomed. Nanotechnol*., 2012, **8**, 125.
9. S. Amini, A. Masic, L. Bertinetti, J. S. Teguh, J. S. Herrin, X. Zhu, H. B. Su and A. Miserez, *Nature Comm*., 2014, DOI: 10.1038/ncomms4187.
10. S. Liu, Y. J. Yin and H. F. Chen, *CrystEngComm*, 2013, **15**, 5853.
11. X. Y. Li, J. X. Zhu, Z. T. Man, Y. F Ao and H. F. Chen, *Sci. Rep.*, 2014, DOI: 10.1038/srep04446.
12. K. P. O'Flynn and K. T. Stanton, *Cryst. Growth Des*., 2012, **12**, 1218.
13. C. L. Chen, Z. C. Wang, M. Saito, T. Tohei, Y. Takano and Y. C. Ikuhara, *Angew. Chem. Int. Ed*., 2014, **53**, 1543.
14. K. Kaneda and T. Mizugaki, *Energy Environ. Sci.*, 2009, **2**, 655.
15. J. K. Liu, J. D. Wang, C. X. Luo and M. Zhang, *J. Nanosci. Nanotechno.*, 2012, **12**, 1924.
16. K. Viipsia, S. Sjöbergb, K. Tõnsuaadua and A. Shchukarevb, *J. Hazard. Mater*., 2013, **252–253**, 91.
17. C. J. Wang, Y. F. Zhang, J. Wei and S. C. Wei, *J. Nanosci. Nanotechno.*, 2012, **12**, 7346.
18. G. B. Ma, X. Y. Liu and M. Wang, *J. Nanosci. Nanotechno*., 2011, **11**, 5199.
19. F. Peng, E. Veilleux, M. Schmidt and M. Wei, *J. Nanosci. Nanotechno*., 2012, **12**, 2774.
20. S. Pushpakanth, B. Srinivasan, T. P. Sastry and A. B. Mandal, *J. Biomed. Nanotechnol*., 2008, **4**, 62.
21. R. J. Wiglusz, A. Kedziora, A. Lukowiak, W. Doroszkiewicz and W. Strek, *J. Biomed. Nanotechnol*., 2012, **8**, 605.
22. T. Mitsudome, S. Arita, H. Mori, T. Mizugaki, K. Jitsukawa and K. Kaneda, *Angew. Chem. Int. Ed*., 2008, **47**, 7938.
23. T. Mitsudome, Y. Mikami, H. Mori, S. Arita, T. Mizugaki, K. Jitsukawa and K. Kaneda, *Chem. Commun*., 2009, **22**, 3258.
24. M. Diaz, F. Barba, M. Miranda, F. Guitian, R. Torrecillas and J.S. Moya, *J. Nanomater*., 2009, **2009**.
25. N. Rameshbabu, T. S. Sampath Kumar, T. G. Prabhakar, V. S. Sastry, K. Murty and K. P. Rao, *J. Biomed. Mater. Res., Part A*, 2007, **80**, 581.
26. G. Ertl, H. Knozinger and J. Weitkamp, Wiley/VCH, Weinheim, 1999.
27. S. Lingamurthy, V. Bhanumathi and B. Sethuram, *J. Phoyoch. Photobio. A*, 1992, **68**, 395.
28. H. Chen, K. Sun, Z. Tang, V. L. Robert, F. M. John, C. J. Agata and B. H. Clarkson, *Cryst. Growth Des*., 2006, **6**, 1504.
29. H. G. Zhang, Q. S. Zhu and Y. Wang, *Chem. Mater*., 2005, **17**, 5824.
30. D. Jiang, D. Li, J. Xie, J. Zhu, M. Chen, X. Lü and S. Dang, *J. Colloids Interface Sci*., 2010, **350**, 30.
31. J. Shen, W. Shan, Y, Zhang, J. Du, H. Xu, K. Fan, W. Shen and Y. Tang, *J. Catal*., 2006, **237**, 94.
32. R. Yamamoto, Y. Sawayama, H. Shibahara, Y. Ichihashi, S. Nishiyama and S. Tsuruya, *J. Catal*., 2005, **234**, 308.
33. Y. Ichikawa, S. Ogata, T. Torimoto, G. Kawachi, K. Kikuta and C. Ohtsuki, *J. Ceram. Soc. Jpn*., 2009, **117**, 294.
34. P. Saravanan, M. P. Raju and S. Alam, Mater. *Chem. Phys*., 2007, **103**, 278.
35. D. Fornasiero and F. Grieser, *J. Colloid Interface Sci*., 1991, **141**, 168.
36. Link and M. A. El-Sayed, *J. Phys. Chem. B*, 1999, **103**, 8410.